

# Synthesis and Characterization of Molecularly Imprinted Poly(methacrylic acid)/Silica Hybrid Composite Materials for Selective Recognition of Lincomycin in Aqueous Media

Yun-Kai Lv, Li-Min Wang, Shuai-Lei Yan, Xiao-Hu Wang, Han-Wen Sun

College of Chemistry and Environmental Science, Hebei University, Key Laboratory of Analytical Science and Technology of Hebei Province, Baoding 071002, China

Received 4 October 2011; accepted 10 January 2012

DOI 10.1002/app.36795

Published online in Wiley Online Library (wileyonlinelibrary.com).

**ABSTRACT:** A novel molecular imprinting method for the preparation of molecularly imprinted poly(methacrylic acid)/silica hybrid composite materials (MIP-HCMs) for the selective recognition of lincomycin (LIN) in aqueous media by prepolymerization and free-radical copolymerization was investigated. In this study, methacrylic acid was selected as the functional monomer, methacryloxypropyltrimethoxysilane was used as the crosslinker, and tetraethoxysilane was used as the inorganic precursor. MIP-HCM was characterized by FTIR spectroscopy, the Brunauer–Emmett–Teller method, and TGA. The selectivity of the sorbent was investigated by

a batch competitive binding experiment with an aqueous LIN and clindamycin (CLI) mixture. The selectivity coefficient for LIN in the presence of CLI was 6.27, whereas the relative selectivity coefficient between LIN and CLI was 5.83. The absorption capability of MIP-HCM and the selectivity coefficient were much higher than those of the nonimprinted blank polymer. © 2012 Wiley Periodicals, Inc. *J. Appl. Polym. Sci.* 000: 000–000, 2012

**Key words:** adsorption; copolymerization; molecular imprinting

## INTRODUCTION

The molecular imprinting technique (MIT) is an increasingly developed technique for preparing polymers with desired and predetermined selectivities and provides specific binding sites or catalytic sites in molecularly imprinted polymers (MIPs).<sup>1</sup> MIPs have attracted wide attention and have been used extensively in sensors,<sup>2</sup> immunoassay-type binding assays in place of antibodies,<sup>3</sup> and separation techniques, which involve affinity chromatography,<sup>4</sup> capillary electrochromatography,<sup>5</sup> solid-phase extraction,<sup>6</sup> thin-layer chromatography,<sup>7</sup> and membrane separation.<sup>8</sup> Organic polymer-based MIPs have been applied extensively because of their excellent pH stability and the easy availability of various monomers, but they may shrink or swell when they are exposed to different organic

solvents and, thus, may cause considerable deformation of the MIP receptors and decrease the recognition ability toward the template.<sup>9,10</sup> Organic–inorganic MIPs have been extensively studied because the inorganic matrix can offer excellent mechanical strength and good solvent resistance. However, hybrid-based MIPs are often prepared with organic metal alkoxide as a functional monomer by a conventional hydrolytic sol–gel process, which often requires curing and aging at high temperature and, thus, inevitably results in poor properties of the MIPs because of the cracking and shrinkage of the MIPs.<sup>11–14</sup>

For these reasons, an alternative approach is the synthetic method of hybrid composite materials (HCMs) combined with the MIT to prepare molecularly imprinted organic–inorganic hybrid composite materials [HCM-based MIPs or molecularly imprinted poly(methacrylic acid)/SiO<sub>2</sub> hybrid composite materials (MIP-HCMs)] at the molecular level. This leads to sufficient compatibility between the organic and inorganic phases in the MIP-HCMs. The obtained materials are more compact and stable. Also, for these copolymers, the ratio of the inorganic and organic components can be conveniently adjusted during polymerization.<sup>15,16</sup> Hence, hybrid materials with flexible compositions and properties, high adsorption capacities, and fast kinetic binding on the template molecules can be obtained.

Correspondence to: Y.-K. Lv (lvyun kai@hbu.edu.cn).

Contract grant sponsor: Hebei Provincial Key Basic Research Program; contract grant number: 10967126D.

Contract grant sponsor: Natural Science Foundation of Hebei Province; contract grant number: B2011201081.

Contract grant sponsor: Scientific Research Foundation of Hebei Provincial Education Department; contract grant numbers: 2008307, 2006407.

In this study, we chose lincomycin (LIN) as the template, methacrylic acid (MAA) as the organic functional monomer, tetraethoxysilane (TEOS) as the inorganic precursor, and methacryloxypropyltrimethoxysilane (KH570) as the coupling agent, which was used to form covalent bonding between the organic and inorganic phases. An LIN-imprinted poly(methacrylic acid) (PMAA)/SiO<sub>2</sub> hybrid composite material (MIP-HCM) was synthesized and characterized. The selectivity and binding properties of the sorbent were investigated by a binding experiment.

## EXPERIMENTAL

### Materials and reagents

LIN and clindamycin (CLI) were purchased from Changheng Biological Pharmaceutical Products Institute (Wuhan, China). MAA was purchased from Tianjin Chemical Reagent Research Institute (Tianjin, China) and cleaned to remove the inhibitor before polymerization. 2,2-Azobisisobutyronitrile (AIBN) was obtained from Beijing Chemical Reagent Co. (Beijing, China) and recrystallized from methanol before use. KH570 and TEOS were supplied by Nanjing Lianye Chemical Co., Ltd. (Shanghai, China). All of the other chemicals used were analytical grade and used without further purification which were applied by Tianjin Regent Chemicals Co., Ltd (Tianjin, China). Doubly deionized water was used throughout.

### Preparation of the LIN-imprinted PMAA/SiO<sub>2</sub> hybrid composite materials

LIN (0.06 g, 0.13 mmol) and MAA (0.1 mL, 1.16 mmol) were dissolved in methanol (4 mL) in a 25-mL, thick-walled glass tube and incubated for 1 h. Then, 0.26 mL of KH570 and 0.01 g of AIBN were added. After the mixture was sonicated for 2 min and purged with nitrogen gas for 5 min, it was stirred for 3 h at 53.8°C. Subsequently, a TEOS solution (TEOS was dissolved in HCl and methanol and stirred for 1 h) was added to the prepolymer solution. The solution was stirred at 50°C for 3 h before it was dried at 65°C.

The obtained MIP-HCM was crushed, ground, and sieved to obtain regularly sized particles between 38.5 and 63 μm before the MIP-HCM particles were extracted with a mixture of methanol and acetic acid (4 : 1 v/v) in a Soxhlet extractor (Tianjin Tianbo Glass Instrument Co., Ltd China) for 3 days to remove the template molecules. After they were washed and dried *in vacuo* at 60°C, the MIP-HCM particles were stored at ambient temperature until use. A nonimprinted blank polymer (NIP) was prepared and treated in an identical manner but in the absence of templates.

### Swelling analysis

The swelling experiments were performed in distilled water. The water uptake was calculated by measurement of the weights of the polymers as follows. Dry MIP-HCM particles with different ratios of MAA to TEOS were carefully weighed ( $\pm 0.0001$  g) and placed in a 2-mL microtube. The microtubes were filled with 1.5 mL of water, sealed with parafilm, and shaken vigorously for 2 min. Subsequent to 6 h of equilibration at 20°C, the weight of the wet sample was measured after the solvent was removed by blotting with moist filter paper. The swelling ratio ( $S_r$ ) of each polymer was calculated from the following equation:

$$S_r(\%) = [(m_s - m_0)/m_0] \times 100\% \quad (1)$$

where  $m_s$  is the mass of the swollen polymer and  $m_0$  is the mass of the dry polymer. Each experiment was carried out in triplicate.

### Determination of the binding properties of the MIP-HCMs

LINs with different masses were added to water (3 mL) to form a series of different concentrations of substrate solution; then, dry MIP-HCM and NIP (30 mg) were added, respectively. The flasks that were filled with the mixtures were incubated under agitation in a horizontal shaker at 25°C for 12 h. These solutions were centrifuged, and the free concentration of LIN after adsorption was measured by ultraviolet–visible spectrophotometry (Beijing purkinje general instrument Co., Ltd. China). The equilibrium adsorption capacity ( $Q$ ) was calculated according to the following equation:

$$Q = V(C_0 - C_e)/m \quad (2)$$

where  $V$  is the volume of solution (mL);  $C_0$  and  $C_e$  are the initial and the equilibrium concentrations of LIN in aqueous media, respectively; and  $m$  is the mass of the sorbent.

### Determination of the selectivity of the MIP-HCMs

To investigate the selectivity of the MIP-HCMs, 30 mg of dry MIP-HCM and NIP particles were added to a 10-mL flask containing a mixed solution of LIN and CLI, whose concentrations were 0.8 mg/mL. Then, the flask was properly sealed, and the mixture was incubated under agitation in a horizontal shaker at 25°C for 12 h. The solution was centrifuged, and the free concentration of LIN after adsorption was measured by ultraviolet–visible spectrophotometry.

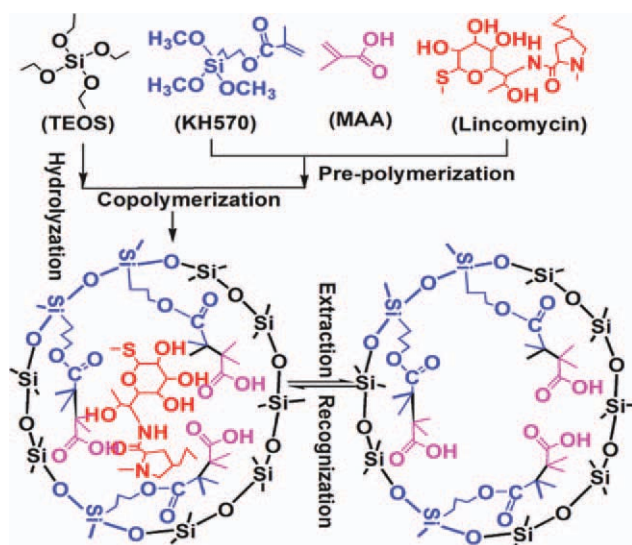


**Figure 1** Synthesis protocol of the LIN-imprinted PMAA/SiO<sub>2</sub> hybrid composite materials and recognition mechanism. [Color figure can be viewed in the online issue, which is available at [wileyonlinelibrary.com](http://wileyonlinelibrary.com).]

## RESULTS AND DISCUSSION

### Synthesis and evaluation of the MIP-HCMs

To prepare the MIP-HCMs, LIN was dissolved in methanol, and MAA was selected as the functional monomer because it was favorable for producing hydrogen-bonding interaction in the solvent. Thus, a stable donor–receptor complex between the template and the functional monomer was formed in the pre-polymerization process.<sup>14</sup> The existence of such a complex led to the formation of well-defined specific binding sites in the polymers. After AIBN was added to the previous complex solution, the prepolymer was synthesized by the copolymerization of MAA and KH570. When the prepolymer solution was mixed with the TEOS hydrolysis solution, a MIP-HCM was prepared. After removal of the template molecule, the specific imprinting sites were maintained. The possible preparation protocol of the MIP-HCMs and the recognition mechanism are shown in Figure 1.

As shown in Table I, the change in the molar ratio of the inorganic precursor to the organic functional monomer caused a remarkable alteration in the adsorption capacity. The inorganic precursor was employed to improve the structural order and mechanical strength of the MIP-HCMs, whereas the

**TABLE I**  
Influence of the MAA/TEOS Ratio on  $Q$  and  $S_r$

MAA/TEOS	$Q$ (mg/g)	$S_r$ (%)
1 : 5	23.47	35.32
1 : 10	48.68	17.46
1 : 15	32.16	12.79

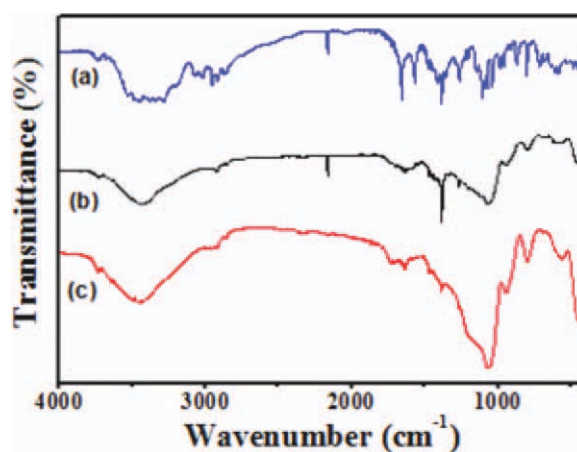


**Figure 2** FTIR spectra of (a) LIN, (b) MIP-HCM (with template), and (c) MIP-HCM (without template). [Color figure can be viewed in the online issue, which is available at [wileyonlinelibrary.com](http://wileyonlinelibrary.com).]

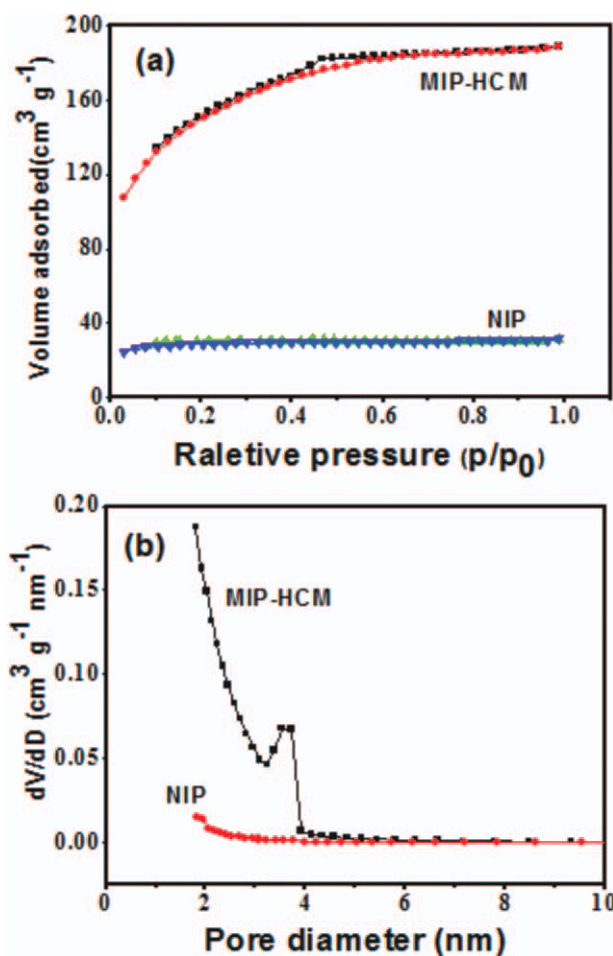


**Figure 3** (a) N<sub>2</sub> adsorption–desorption isotherms and (b) the corresponding pore size distributions of MIP-HCM and NIP.  $p$  is the pressure of experiment,  $P_0$  is atmospheric pressure, and  $Dv/Dd$  is the ratio of pore volume to pore diameter. [Color figure can be viewed in the online issue, which is available at [wileyonlinelibrary.com](http://wileyonlinelibrary.com).]

TABLE II  
Porosimetry of the MIP-HCMs and NIP

	Surface area (m <sup>2</sup> /g)	Pore volume (cm <sup>3</sup> /g)	Pore size (nm)
MIP-HCMs	527.02 ± 8.02	0.292	2.22
NIP	93.57 ± 2.39	0.048	2.06

organic functional monomer controlled the active groups of the template cavity. When the molar ratio of MAA to TEOS was 1 : 10, the polymer exhibited a higher uptake capacity (48.68 mg/g) for LIN.

Meanwhile, the change in the molar ratio of the inorganic precursor to the organic functional monomer altered the  $S_r$  value of the MIP-HCMs. The result of swelling analysis can be seen in Table I. With increasing mechanical strength, the uptake of the MIP-HCMs for solvent was limited.

FTIR spectroscopy (Nicolet 380 FT-IR, Thermo Electron Corporation, USA) is an important physical method for determining the structure of MIP-HCMs. Figure 2 shows the IR spectra of LIN, MIP-HCM (with template), and MIP-HCM (without template). From the curve in Figure 2(b), we found a strong and broad stretching vibration absorbance peak of hydroxyl groups at 3455 cm<sup>-1</sup>; this suggested that there were a few hydroxyl groups in the polymers because the added amounts of TEOS may not have corresponded necessarily to the amounts of SiO<sub>2</sub> formed after the sol-gel reaction.<sup>14</sup> At 797, 461, and 1066 cm<sup>-1</sup>, the weak absorbance peak of Si-O and Si-O-C indicated the formation of a binding between the inorganic precursor and the organic functional monomer which were not simply physically mixed.<sup>16</sup> In the curve in Figure 2(c), the C-N

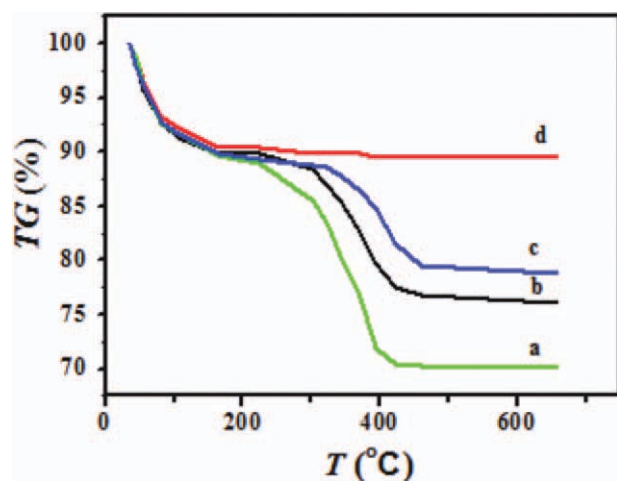


Figure 4 Thermogravimetric weight loss curves of the materials from different ratios of MAA to TEOS: (a) 1 : 5, (b) 1 : 10, (c) 1 : 15, and (d) SiO<sub>2</sub>. TG is the ratio of the loss weight, and T is the temperature of the analysis. [Color figure can be viewed in the online issue, which is available at wileyonlinelibrary.com.]

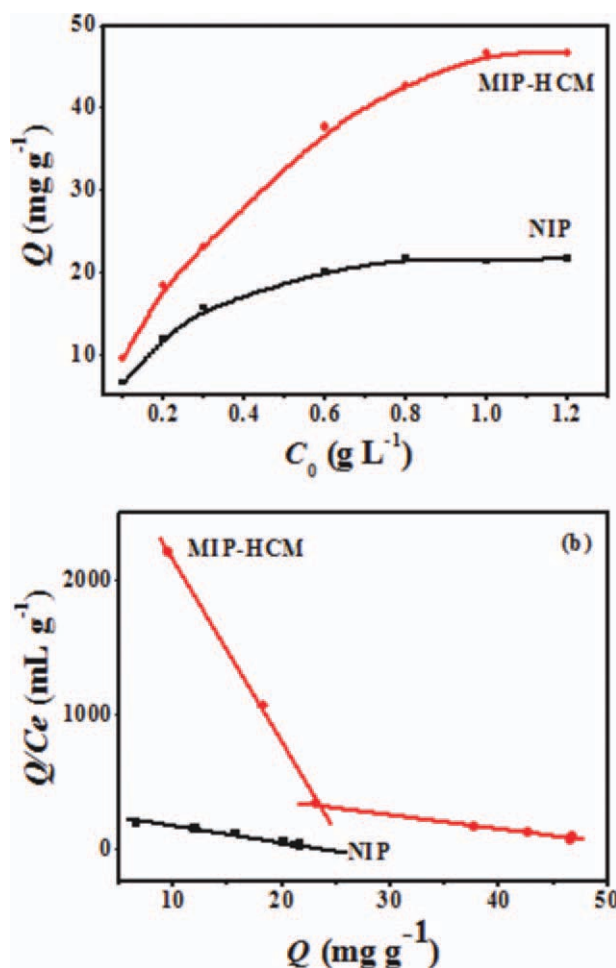
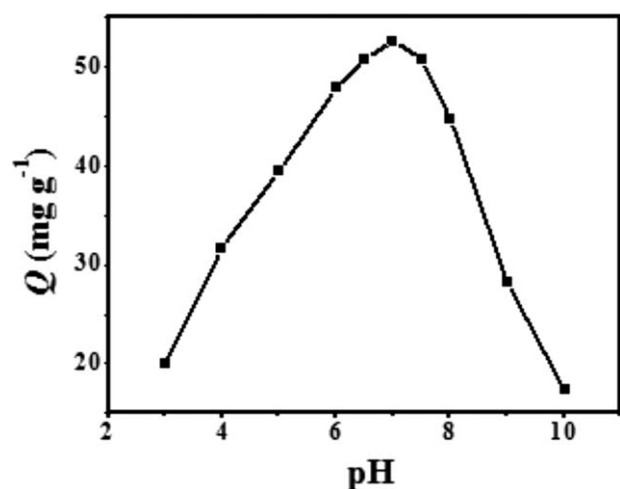


Figure 5 (a) Binding isotherm and (b) Scatchard plot analysis of the binding of LIN onto MIP-HCM. [Color figure can be viewed in the online issue, which is available at wileyonlinelibrary.com.]

peak (at 1386 cm<sup>-1</sup>) disappeared, and we inferred that the template molecules of MIP-HCM were eluted cleanly from the cavities.

The pore structure, surface area, and Brunauer-Emmett-Teller isotherms were studied with nitrogen adsorption-desorption experiments. The N<sub>2</sub> adsorption-desorption isotherms and pore-size distributions of the MIP-HCMs and NIP are shown in Figure 3. The MIP-HCM isotherms presented type IV curves with one well-defined step at an intermediate partial pressure related to the capillary condensation of N<sub>2</sub> inside the mesopores, whereas the NIP isotherms showed type I curves. Meanwhile, the MIP-HCMs also showed narrow pore-size distributions [Fig. 3(b)]. The parameters related to the products are summarized in Table II. The MIP-HCMs presented higher Brunauer-Emmett-Teller surface areas and bigger pore volumes than the NIP. One reason for this phenomenon was that the MIP-HCMs had more binding sites because of the effect of the template molecule.



**Figure 6** Adsorptive capacity of MIP-HCM in solution with different pH values.

Figure 4 shows the results of differential thermogravimetric analysis of the MIP-HCMs with different molar ratios of MAA to TEOS. The MIP-HCMs appeared to decrease slightly at 220°C due to the removal of the adsorbed water and solvent, whereas the major weight loss of the polymer was attributed to the decomposition of the polymers. The temperature at which the MIP-HCMs presented an abrupt decrease in weight rose with decreasing MAA/TEOS. The thermal stabilities of the hybrid polymers were improved with decreasing MAA/TEOS because the ordered alignment of the polymer chain was melded by the crosslinking between the inorganic precursor and the organic functional monomer; this delayed and prevented the thermal decomposition of the polymers.<sup>15</sup>

### Adsorption studies

The adsorption of LIN by MIP-HCM was studied at different initial LIN solution concentrations (0.2–1.0 mg/mL). As shown in Figure 5(a), the adsorption capacity of MIP-HCM increased from 9.6 to 46.7 mg/g with the concentration of LIN, whereas that of NIP increased from 6.6 to 21.7 mg/g. As the equilibrium adsorptive amount of the MIP-

HCMs was larger than that of NIP, we inferred that the MIP-HCMs had more binding sites and larger pore sizes with the effect of molecular imprinting.

In general, Scatchard plotting is used for the evaluation of adsorption parameters. Furthermore, a Scatchard plot can indicate how many kinds of binding sites exist, for example, in the MIP-HCMs. The average binding data of triplicate independent results were linearly transformed according to the Scatchard equation [ $Q/C_e = (Q_{\max} - Q)/K_d$ , where  $Q_{\max}$  is the apparent maximum binding capacity and  $K_d$  is the equilibrium dissociation constant]. The results indicate that there were two different binding sites in the MIP-HCMs and only one kind of binding site for the NIP, as shown in Figure 5(b). The fitting liner equations for the MIP-HCMs were  $Q/C_e = 3532.12 - 137.03Q$  and  $Q/C_e = 590.76 - 11.08Q$  with  $K_d$ 's of  $7.3 \times 10^{-3}$  and  $9.02 \times 10^{-2}$  mg/mL, respectively, and  $Q_{\max}$  values of 25.77 and 53.31 mg/g, respectively, were calculated from the slope and the intercept of the linear equation. Similarly,  $K_d$  ( $8.8 \times 10^{-2}$  mg/mL) and  $Q_{\max}$  (24.42 mg/g) values were calculated from the fitting liner equation ( $Q/C_e = 277.01 - 11.34Q$ ) for the NIP [Fig. 4(b)]. This indicated that the specific affinity and the binding capacity of the MIP-HCMs were significantly larger in comparison with those of the NIP.

The effect of the solution pH on the equilibrium adsorption amount is shown in Figure 6. It is shown that the MIP-HCMs had the best adsorption (52.6 mg/g) in the solution with pH 7. The interactions between the LIN and MIP-HCMs became stronger because of protonation; when the pH was lower than 7, the adsorption increased with increasing pH. However, the adsorption decreased with increasing pH when the pH was higher than 7 because the MAA was resolved, and the MIP-HCMs lost the binding site.

### Selectivity of the MIP-HCMs

The selective adsorption of the MIP-HCMs was evaluated with LIN and its structurally similar compound (CLI) in water at pH 7. The static

**TABLE III**  
Competitive Loading of LIN and CLI by the MIP-HCMs and NIP

Sorbent	Initial solution (mg/mL)		Uptake (%)		Capacity (mg/g)		$K_D$ (mL/g) <sup>a</sup>		$K^b$	$k^c$
	LIN	CLI	LIN	CLI	LIN	CLI	LIN	CLI		
MIP-HCMs	0.8	0.8	60.5	19.6	48.4	15.7	153.2	24.4	6.27	5.83
NIP	0.8	0.8	22.8	21.5	18.2	17.2	29.4	27.4	1.08	

<sup>a</sup>  $K_D$  is the ratio of the mass of LIN absorbed per gram of sorbent to the concentration of LIN in the final solution.

<sup>b</sup>  $K = K_{D(LIN)}/K_{D(CLI)}$ .

<sup>c</sup>  $k' = k_{MIP}/k_{NIP}$ .

adsorption distribution coefficient ( $K_D$ ) was used to evaluate the molecular selectivity of the polymers.<sup>11</sup> Table III shows the  $K_D$ , selectivity coefficient ( $K$ ), and relative selectivity coefficient ( $k'$ ) values. We observed that the adsorption capacities of NIP were very close for both LIN and CLI because there were not specific recognition sites in the NIP, and the adsorption for substrates was nonselective. On the other hand, obviously, the MIP-HCMs offered better selectivity for LIN because the MIPs presented a  $K$  value about 5.8 times that of the corresponding NIP. This may have been due to the flexibility of the cavity and which specific binding sites contained functional groups in a predetermined orientation.

### CONCLUSIONS

We have demonstrated successful fabrication of a new molecularly imprinted organic–inorganic hybrid composite material in this study. By coupling MIT to hybrid composite synthesis technology and sol–gel technology, with this method, we provided flexible reaction conditions, which could improve the adsorption capacity, selectivity, and thermal stability. We expect that the synthesis and application protocol of molecularly imprinted organic–inorganic hybrid composite materials is promising as a general

strategy for the fabrication of highly selective imprinted hybrid composite materials.

### References

1. Haupt, K. *Analyst* 2001, 126, 747.
2. Bompart, M.; De Wilde, Y.; Haupt, K. *Adv Mater* 2010, 22, 2343.
3. Tang, P. P.; Luo, Z. F.; Cai, J. B.; Su, Q. D. *Chin J Anal Chem* 2010, 38, 1019.
4. Guerreiro, A. R.; Chianella, I.; Piletska, E.; Whitcombe, M. J.; Piletsky, S. A. *Biosens Bioelectron* 2009, 24, 2740.
5. Lämmerhofer, M.; Gargano, A. *J Pharm Biomed Anal* 2010, 53, 1091.
6. Lucci, P.; Derrien, D.; Alix, F.; Pérollier, C.; Bayouduh, S. *Anal Chim Acta* 2010, 672, 15.
7. Suedee, R.; Songkram, C.; Petmoreekul, A.; Sangkunakup, S.; Sankasa, S.; Kongyart, N. *J Pharm Biomed Anal* 1999, 19, 519.
8. Chen, J. H.; Li, G. P.; Liu, Q. L.; Ni, J. C.; Wu, W. B.; Lin, J. M. *Chem Eng J* 2010, 165, 465.
9. Wang, H. F.; Zhu, Y. Z.; Lin, J. P.; Yan, X. P. *Electrophoresis* 2008, 29, 952.
10. Tamayo, F. G.; Turiel, E.; Martín-Esteban, A. *J Chromatogr A* 2007, 1152, 32.
11. Lu, Y. K.; Yan, X. P. *Anal Chem* 2004, 76, 453.
12. Diaz-Garcia, M. E.; Laino, R. B. *Microchim Acta* 2005, 149, 19.
13. Adam, K.; Michal, P.; Wojciech, C.; Jacek, N. *Crit Rev Anal Chem* 2010, 40, 172.
14. Zhang, Z. H.; Zhang, H. B.; Hu, Y. F.; Yao, S. Z. *Anal Chim Acta* 2010, 661, 173.
15. Ahmad, Z.; Mark, J. E. *Chem Mater* 2001, 13, 3320.
16. Wu, Y. H.; Wu, C. M.; Xu, T. W.; Fu, Y. X. *J Membr Sci* 2009, 329, 236.